Available online at www.sciencedirect.com
SCIENCE DIRECT®
Precambrian Research 134 (2004) 275–292
Precambrian Research
www.elsevier.com/locate/precamres

Evolution of the continental crust in the Kerala Khondalite Belt, southernmost India: evidence from Nd isotope mapping, U–Pb and Rb–Sr geochronology

Bénédicte Cenki[a,b], Ingo Braun[a,*], Michael Bröcker[b]

[a] *Mineralogisch-Petrologisches Institut, Universität Bonn, Poppelsdorfer Schloβ, D-53115 Bonn, Germany*
[b] *Institut für Mineralogie, Zentrallaboratorium für Geochronologie, Universität Münster, Corrensstr. 24, D-48149 Münster, Germany*

Received 6 December 2002; accepted 23 June 2004

Abstract

In order to decipher crustal genesis and evolution as well as to refine the metamorphic history of the Kerala Khondalite Belt (KKB), southernmost India, we have applied U–Pb monazite, Rb–Sr biotite-feldspar dating and Nd isotope geochemistry. The KKB belonged to an eastern Gondwana mobile belt that underwent ultra-high temperature metamorphism at Pan-African times. It is dominated by Nd model ages ranging between 2.0 and 3.0 Ga except at its northernmost boundary (the Achankovil Unit, AU), where Middle Proterozoic Nd model ages were recognised (1.3–1.6 Ga). The new data show, that these ages are not restricted to cordierite-bearing metasediments alone but can be found in other lithologies of the Achankovil Unit as well. Peak metamorphism occurred between 590 and 550 Ma as recorded by U–Pb dating of monazite from charnockites and garnet-biotite gneisses. Rb–Sr ages of minerals in pegmatite intrusions record cooling to ca. 400–500 °C by 490-470 Ma. Based on a systematic regional sampling, this contribution confirms and refines former models based on smaller datasets. The major issue is that the Kerala Khondalite Belt must have undergone an extremely slow cooling history (3–6 °C/Ma) comparable to the one described for Sri Lanka and Madagascar. Still such ultra-high temperatures associated to slow cooling processes cannot be satisfactorily fit into a common tectonic context.

Keywords: Kerala Khondalite Belt; Nd model ages; Monazite dating; Rb–Sr age; Ultra-high temperature metamorphism

1. Introduction

During the Pan-African orogeny (ca. 500–700 Ma) and assembly of East and West Gondwana the Proterozoic part of Peninsular India was located close to Sri Lanka, southern Madagascar and East Antarctica (e.g. Lawver and Scotese, 1987; Powell et al., 1988;

* Corresponding author.
E-mail addresses: bcenki@yahoo.fr (B. Cenki), ingo.braun@uni-bonn.de (I. Braun).

0301-9268/$ – see front matter © 2004 Published by Elsevier B.V.
doi:10.1016/j.precamres.2004.06.002

Kriegsman, 1995; Fitzsimons, 2000; Collins and Windley, 2002). Similarities in tectonic style, degree of metamorphism and age patterns suggest that these terranes most likely shared a common tectono-metamorphic evolution (e.g. Nicollet, 1990; Hiroi and Motoyoshi, 1990; Yoshida et al., 1992; Ghosh, 1999; Fitzsimons, 2000; De Wit et al., 2001). However, the absence of systematic isotope geochemical and geochronological datasets for the crystalline basement of southern India as well as insufficient correlation between structural, petrological and geochemical studies has prevented to develop a better understanding of the Proterozoic tectono-metamorphic evolution of southern India and its position within East Gondwana.

In order to shed some light on the crustal genesis and the metamorphic history of the Kerala Khondalite Belt (KKB), we carried out geochemical and geochronological investigations on a set of samples which represents the lithological make-up of this lower crustal terrain fairly well. The Nd isotope composition of whole rock samples was analysed to distinguish crustal terrains of different origin, U–Pb ages of monazites were determined to establish the age of peak metamorphism and Rb–Sr dating of biotite and feldspar from pegmatites was carried out in order to constrain the late stage of the metamorphic evolution.

2. Geological setting

2.1. Geological setting and previous geochronological studies

The Pan-African orogen of southernmost India is separated from the Archean and Early Proterozoic crystalline basement by the Palghat-Cauvery Shear Zone (PCSZ) and associated shear zone systems (Fig. 1a). It is commonly divided into the Madurai Block (MB) and the KKB which are separated by the Achankovil Unit (AU; Drury and Holt, 1980; Drury et al., 1984). The KKB (Srikantappa et al., 1985) encloses, from north to south, the AU, the Ponmudi Unit (PU) and the Nagerkoil Unit (NU; Fig. 1b). The PU and the AU consist of garnet-biotite gneisses and garnet ± biotite ± cordierite ± sillimanite ± graphite gneisses representing a supracrustal sequence of pelitic and psammitic origin (Chacko et al., 1992). They were intruded by early granitoid rocks that were migmatised and transformed into augen gneisses and fine-grained biotite-bearing gneisses during the Pan-African orogeny. The NU is mostly composed of massive charnockites, enderbites and mafic granulites (Srikantappa et al., 1985). It thus has long been considered as a distinct block with a distinct tectonic and metamorphic evolution (Chacko et al., 1996; Santosh, 1996). The MB is predominantly composed of massive charnockites and enderbites as well as hornblende ± biotite gneisses interpreted as a volcano-sedimentary sequence.

The entire area underwent ultra-high temperature metamorphism (Chacko et al., 1996; Satish Kumar and Harley, 1998; Nandakumar and Harley, 2000; Cenki et al., 2002) at Pan-African times (Buhl, 1987; Choudhary et al., 1992; Soman et al., 1995; Miller et al., 1997; Bartlett et al., 1998). The metamorphic evolution of the KKB is characterised by a clockwise PT path with post-peak isobaric cooling followed by isothermal decompression (Satish Kumar and Harley, 1998; Nandakumar and Harley, 2000; Fonarev et al., 2000; Cenki et al., 2002). Peak pressure estimates are lower (6–7 kbar; Chacko et al., 1996; Satish Kumar and Harley, 1998; Nandakumar and Harley, 2000; Cenki et al., 2002) than in the MB where sapphirine is locally present and maximum pressures of ca. 10–12 kbar have been reported (Raith et al., 1997; authors' own observations). Recent studies (e.g. Ghosh et al., 1998; Cenki and Kriegsman, unpublished data) presented new structural data and tectonic models for southernmost India and suggested that the whole area is a single tectonic domain. Major differences between the various units of the SGT concern their lithology as well as the age and nature of their protoliths. Geochronological and isotope data suggest that the Pan-African event in Peninsular India was essentially a period of crustal reworking. Nd model ages obtained from gneisses and charnockites in the PU and MB range between 3.0 and 2.0 Ga (Harris et al., 1994; Brandon and Meen, 1995; Bartlett et al., 1998). The boundary between these domains is marked by a ca. 30 km wide zone of much younger Nd model ages (ranging from 1.5 to 1.2 Ga with εNd initial values of −6.0 to −3.1; Brandon and Meen, 1995; Bartlett et al., 1998). This zone is the AU (Braun and Kriegsman, 2003). Similar ages were reported for cordierite gneisses in Kerala and were interpreted to result from mixing of source rocks of Early and Late

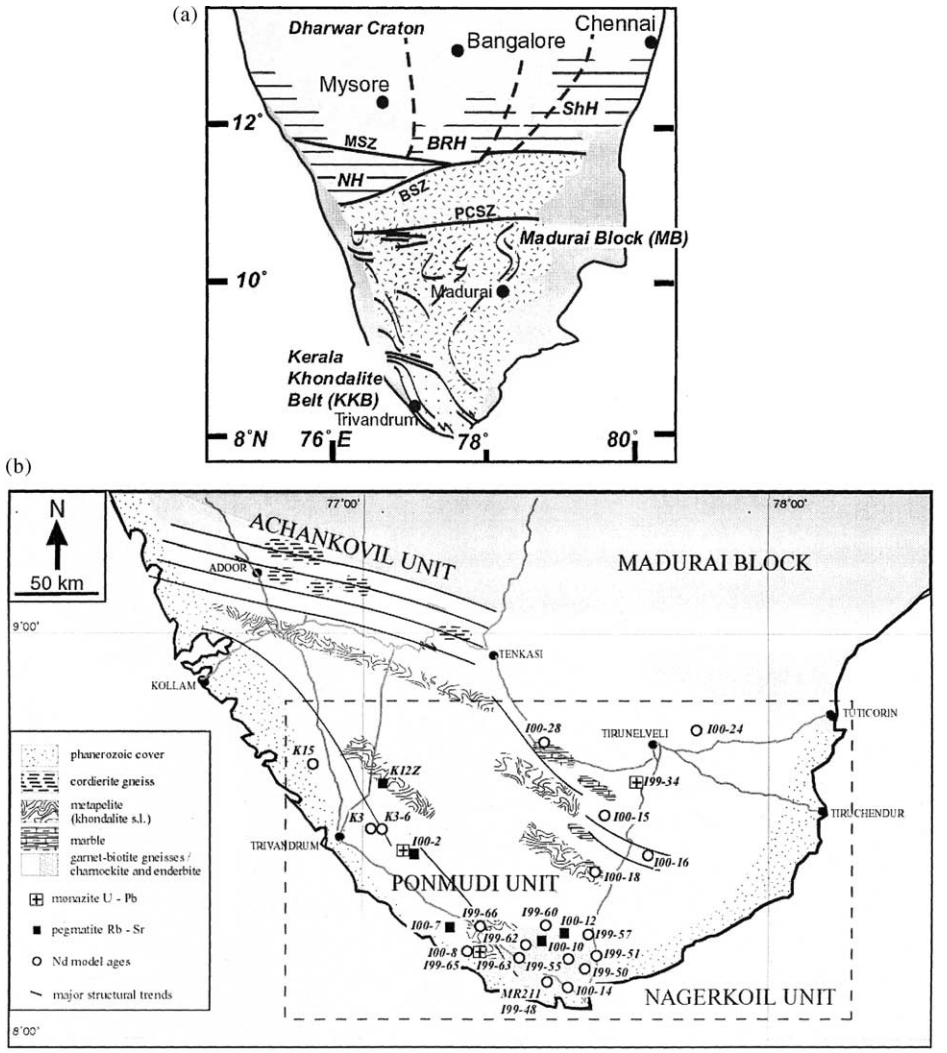

Fig. 1. (a) Simplified geological map of South India (modified after Raith et al., 1997). MSZ: Moyar Shear Zone; BSZ: Bhavani Shear Zone; PCSZ: Palghat-Cauvery Shear Zone; NH: Nilgiri Hills; BRH: Biligirirangan Hills; ShH: Shevaroy Hills. Major structural trends (Cenki and Kriegsman, unpublished data) are indicated in thick black lines. (b) Schematic geological map of the Kerala Khondalite Belt (modified after Braun and Kriegsman, in press). All localities selected for geochronological and isotopic geochemical work in this contribution are indicated. Dashed box shows the domain shown in Figs. 2 and 4.

Proterozoic age (Bartlett et al., 1995), the latter of which are not known from the exposed crust of Peninsular India.

As documented by various geochronological methods, the major tectono-metamorphic event recorded in the KKB is of Pan-African age (560–516 Ma; Buhl, 1987; Choudhary et al., 1992; Soman et al., 1995; Unnikrishnan-Warrier et al., 1995; Miller et al., 1997; Unnikrishnan-Warrier, 1997; Bartlett et al., 1998; Braun et al., 1998; Ghosh, 1999; Braun and Bröcker, 2004). The existence of an Early Proterozoic metamorphic event has been inferred from single zircon Pb-evaporation ages of 1802 ± 16 Ma (Bartlett et al., 1998), the results of electron microprobe dating (EPMA) of monazite from paragneisses (1.9–1.7 Ga; Braun et al., 1998; authors' unpublished

data; Santosh et al., 2003) and a Sm–Nd garnet-whole rock isochron age of ca. 1793 Ma (Choudhary et al., 1992). Ghosh (1999) reported a 987 Ma zircon upper intercept age for a gneiss xenolith in the Kalipara granite. Late Pan-African Rb–Sr cooling ages (484–440 Ma; Choudhary et al., 1992; Unnikrishnan-Warrier et al., 1995; Unnikrishnan-Warrier, 1997) were reported for pegmatites, granitic gneisses and leucogranites. They are in good agreement with K–Ar biotite ages for pegmatites (474–445 Ma, Soman et al., 1982) and EPMA monazite ages of pegmatites and gneisses (520–420 Ma, Braun et al., 1998 and authors' unpublished data; Santosh et al., 2003).

2.2. Sample description

Rock samples selected for this study represent the major rock types of the PU, the AU and the NU and comprise garnet-biotite gneisses, metapelites, charnockites, enderbites and pegmatites. Accounts on their geochemistry and petrology are given elsewhere (e.g. Srikantappa et al., 1985; Chacko et al., 1992; Santosh, 1996; Braun et al., 1996).

The majority of investigated samples comprises migmatitic garnet-biotite gneisses which can be further subdivided into different textural variants. Most of them (I00-16-1; I00-18-2; I99-60-1; I99-51-1; I99-66-9) display a stromatic texture consisting of a garnet-biotite-rich melanosome and a garnet-bearing quartzofeldspathic leucosome. Garnet has a subhedral shape with grain sizes of at least 500 μm. It formed from biotite-dehydration melting according to the reaction biotite + sillimanite + quartz + plagioclase = garnet + K-feldspar + liquid and contains inclusions of relic quartz, K-feldspar, plagioclase, biotite and rare sillimanite. Biotite and cordierite are commonly observed as breakdown products of garnet in metapelitic and metapsammitic rocks (Cenki et al., 2002). Biotite predominantly occurs in the melanosome and is rarely present in the leucosome. It displays a sub- to euhedral shape and defines the gneissic foliation of the rock. The leucosome is mainly composed of quartz, K-feldspar and plagioclase, the amount of which depends on the degree of partial melting and mineral-melt back-reaction (Cenki et al., 2002). Monazite, zircon, apatite, opaque phases and graphite are accessories. Sample K3 represents the group of leptynitic gneisses. The characteristic textural feature of these fine- to medium-grained rocks is a lensoid garnet-bearing leucosome in a biotite-bearing gneiss matrix. In contrast, the augen gneiss sample K15-1 shows a magmatic, porphyritic texture defined by centimetre-sized K-feldspar phenocrysts which are oriented within the foliation plane. They were derived from porphyritic granites which intruded into the crystalline basement of the KKB prior to the peak of Pan-African metamorphism and penetrative deformation (Braun et al., 1998; Braun and Bröcker, 2004). Sample I00-14-2 is a strongly migmatitic metapelite. Compared to the garnet-biotite gneisses, it has higher modal abundances of sillimanite, graphite and cordierite. Leucogranites (K3-6; I99-66-8; I00-18-3) usually occur as centimetric to plurimetric sheets injected along or cross-cutting the foliation of the garnet-biotite gneisses. Garnet and/or sillimanite generally are present with low modal abundances. Accessory phases are almost absent in the studied rocks and comprise zircon, monazite, apatite and ilmenite.

Roughly one-third of the samples selected for Nd isotope studies and half of the samples selected for U–Pb dating are charnockites or enderbites (I00-28-1; I00-24-1; I00-15-5b; I00-15-5a; I99-57-1; I99-62-1; I99-63-3; I99-50-1; I99-55-1; MR211). On outcrop scale, the dark green colour of the rocks suggests a massive appearance and a homogeneous granoblastic texture. However, a closer look in hand specimen often reveals the existence of a stromatic to nebulitic texture. The leucosomes of charnockites are mostly composed of granoblastic quartz, plagioclase and K-feldspar. Enderbites are similar except that they are richer in plagioclase and have lower modal amounts of quartz and K-feldspar. Orthopyroxene is subhedral, slightly pleochroic and rarely poikilitic. It is locally intergrown with biotite, opaque phases and garnet which is interpreted to reflect garnet and orthopyroxene growth from biotite-dehydration melting. Rare biotite commonly fills embayments of orthopyroxene crystals and is thus interpreted as a breakdown product of orthopyroxene (Cenki et al., 2002). Accessory minerals are zircon, apatite, opaque phases, hercynite and graphite. Metabasites (I99-48-2; I99-55-3; I99-50-2) appear as cross-cutting or interlayered dykes in charnockites or enderbites. The major ferromagnesian phase is amphibole. Orthopyroxene, clinopyroxene and opaque phases are present as well. Biotite is rare and commonly fills mafic minerals embayements and thus forms from orthopyroxene or amphibole breakdown

upon hydration. Plagioclase is the main phase in the leucosome, quartz is minor and K-feldspar is absent.

Pegmatites (K12-2; I00-2-2; I00-12-1; I00-10-3; I00-7-2), selected for Rb–Sr dating of biotite and feldspar, occur as dykes of 50–80 cm width, and intruded into charnockites and enderbites. Release of hydrous fluids upon melt crystallisation has led to bleaching of the adjacent granulite and the formation of biotite-bearing gneisses. Generally, the width of this bleaching zone is less than one meter. During this process, orthopyroxene broke down to biotite and a gneissic foliation re-appeared (e.g. Ravindra Kumar and Chacko, 1986; Santosh and Yoshida, 1986). Pegmatites contain large crystals of biotite (<500 μm), K-feldspar, plagioclase and quartz ± apatite, monazite and zircon.

3. Analytical methods

3.1. Isotope geochemistry

Whole rock powders were prepared at Mineralogisches Institut, Universität Bonn by using a steel jaw-crusher and an agate shatter-box. Isotope analyses were carried out at the Zentrallaboratorium für Geochronologie (ZLG) at the Institut für Mineralogie, Universität Münster. In order to ensure complete dissolution of whole rock powders, sample digestion for Sm–Nd studies was carried out in teflon bombs within screw-top steel containers, according to the method suggested by Krogh (1973) for zircon. In a first step, whole rock powders (50–200 mg depending on Sm and Nd concentrations determined by XRF) were mixed with a $^{149}Sm/^{150}Nd$ spike in teflon screw-top vials and dissolved in a HF–HNO3 (5:1) mixture on a hot-plate overnight. The solution was then reduced to a smaller volume by evaporation on a hot-plate and transferred into teflon bombs with fresh HF–HNO3 (5:1). After a few days in steel autoclaves at ca. 200 °C, the dissolved samples were transferred to Savilex screw-top beakers. A few drops of HClO4 were added to break down fluorides during drying on a hot-plate. After complete evaporation, 6N HCl was added to the residue and excess HF and HClO4 removed in a second evaporation step. Bulk REE were separated by standard ion-exchange procedures (AG 50W-X8 resin) on quartz glass columns using 2.5N and 6N HCl as eluants. Sm and Nd were extracted from the REE fraction using teflon powder coated with 2-ethyl-hexyl phosphoric acid and 0.2N and 0.4N HCl as eluant. For mass-spectrometric analysis, Sm and Nd were loaded with HCl on Re filaments using a triple filament configuration. The $^{147}Sm/^{144}Nd$ ratios were assigned uncertainties of 0.3%. Uncertainties of the $^{143}Nd/^{144}Nd$ ratios are reported on the 2σm level. Repeated runs of the LaJolla standard gave an average $^{143}Nd/^{144}Nd$ ratio of 0.511858 ± 15 (n = 7). Fractionation was corrected by normalising the given isotope ratios to $^{146}Nd/^{144}Nd = 0.7219$. Total procedure blank did not exceed 0.05 ng for Nd and 0.02 ng for Sm and are negligible because contents of the samples are usually 1000 times higher at least. εNd at the time of metamorphism (550 Ma) was calculated relative to CHUR with present-day values of $^{143}Nd/^{144}Nd = 0.512638$ and $^{147}Sm/^{144}Nd = 0.1967$ (Jacobsen and Wasserburg, 1980). Nd model ages were calculated assuming a depleted-mantle reservoir and present-day values of $^{143}Nd/^{144}Nd = 0.51315$ and $^{147}Sm/^{144}Nd = 0.217$ (Goldstein et al., 1984). This procedure is based on the assumption that the major chemical fractionation of Sm and Nd took place when the source material was differentiated from depleted mantle prior to its incorporation into the crust (e.g. McCullogh, 1987; Jahn and Condie, 1995). Caution is warranted in the case of highly migmatized rocks because Sm and Nd do not fractionate similarly between melt and restite (Brandon and Meen, 1995). As will be shown in Section 4.2, the studied samples are not affected by this process.

The validity of interpretation of Nd model ages and εNd calculations is always limited by the precision and confidence in measured and calculated values. εNd initial reproducibility based on duplicate dissolutions of samples is always better than 0.4 εNd units. The average difference in the $^{147}Sm/^{144}Nd$ ratio of duplicates is 0.0015. Within-run error for $^{143}Nd/^{144}Nd$ is always under 0.0002. The reproducibility of duplicate analyses from solutions issued from the same chemical procedure is in the range 0.1–1.2 εNd units, a little higher than for separate dissolutions. Within-run precision is better than 0.6 εNd units. Thus model ages reproduce within less than 40 Ma.

3.2. Geochronology

For U–Pb geochronology, monazite was concentrated from the <355 μm size fraction by standard routines using jaw-crusher, disc-mill, magnetic and heavy

liquid techniques. Three to ten grains per size fraction were hand-picked under a binocular microscope according to the following criteria: sub-euhedral, mostly without inclusions, pale yellow, smooth surface. To remove surface contamination, hand-picked monazites were ultrasonically cleaned with diluted high purity HCl and deionised water. Decomposition of monazite followed the procedures suggested by Krogh (1973) for zircon, but using 6N HCl instead of HF for dissolution. For chemical separation of U and Pb a HBr technique was applied. A ^{233}U–^{205}Pb mixed spike was used for isotope dilution. U and Pb were loaded with phosphoric acid and silica gel on single Re filaments and isotope ratios were measured on a VG Sector 54 multicollector mass spectrometer in static mode. Isotopes were usually measured on Faraday cups except for ^{204}Pb which was simultaneously measured with a Daly detector ion counting system. Due to low intensities, ^{205}Pb and ^{207}Pb often had to be analysed with the Daly detector, too. Total procedural blanks did not exceed 140 pg for Pb and 15 pg for U. Isotopic ratios were corrected for mass discrimination with a factor of 0.1% per amu for Pb and U. Reproducibility of the $^{207}Pb/^{206}Pb$ ratio of the standard NBS-982 was <0.045%. For initial lead correction, isotopic compositions calculated according to the model of Stacey and Kramers (1975) were employed. All ages and error ellipses were calculated using the Isoplot program, version 2.49 (Ludwig, 1991).

For Rb–Sr geochronology five pegmatite samples were selected. Centimeter-sized biotite flakes were split from the hand specimen by the use of a knife. Possible contaminants located between individual mica sheets were removed by grinding under ethanol in an agate mortar. A felsic fraction representing a mixture of plagioclase and K-feldspar was obtained by hand-picking. Mica concentrates (optically pure >99%) were washed in ethanol (p.a.) and deionized H2O in an ultrasonic bath. For Rb–Sr analyses, feldspar (ca. 50 mg) and biotite (ca. 40 mg) were mixed with a $^{87}Rb/^{84}Sr$ spike in teflon screw-top vials and dissolved in a HF–HNO3 (5:1) mixture on a hot-plate overnight. After drying, 6N HCl was added to the residue. This mixture was homogenised on a hot-plate overnight. After a second evaporation to dryness, Rb and Sr were separated by standard ion-exchange procedures (AG 50W-X8 resin) on quartz glass columns using 2.5N and 6N HCl as eluants. For mass-spectrometric analysis, Rb was loaded on Ta filaments (double filament) with H2O. Sr was analysed using TaF5 on W filaments (single filament). Mass-spectrometric analysis was carried out using a VG Sector 54 multicollector mass spectrometer (Sr) and a NBS-type Teledyne mass spectrometer (Rb). Correction for mass fractionation is based on a $^{86}Sr/^{88}Sr$ ratio of 0.1194. Rb ratios were corrected for mass fractionation using a factor deduced from multiple measurements of NBS-607. Total procedural blanks were less than 0.05 ng for Rb and 0.20 ng for Sr. Based on repeated measurements, an uncertainty of 1% (2σ) is usually assigned to the $^{87}Rb/^{86}Sr$ ratios. However, analytical problems resulted in an uncertainty of up to 2% for some of the studied samples. Still, the error in age is acceptable for a regional scale study. For the $^{87}Sr/^{86}Sr$ isotope ratio uncertainties represent the within-run statistics (2σ). Repeated runs of standard NBS-987 gave an average $^{87}Sr/^{86}Sr$ ratio of 0.710292 ± 18 (2σ, n = 10). All ages were calculated using the IUGS recommended decay constants (Steiger and Jäger, 1977) by means of a ZLG program and the Isoplot program version 2.49 (Ludwig, 1991).

4. Results

4.1. Nd isotope data

In order to complement the Nd isotope dataset available for the KKB (see compilation in Braun and Kriegsman, 2003), this study has focussed on the NU (Fig. 1b) and its presumed transition to the PU. For comparison, a limited number of samples from representative localities of the PU and AU were also analysed. Sm–Nd isotope results are presented in Table 1 and Fig. 2. The studied samples show a wide range of Sm and Nd concentrations (0.4–17 ppm and 16–103 ppm, respectively). $^{147}Sm/^{144}Nd$ ratios display typical crustal values (0.07–0.12) indicating that no major Sm/Nd fractionation took place during high-grade metamorphism. Exceptions are two metabasites (I99-48-2 and I99-55-3) with $^{147}Sm/^{144}Nd$ ratios up to 0.15. Initial εNd values, corrected for in situ decay of ^{147}Sm, were calculated for t = 550 Ma, which is considered to be a reasonable minimum estimate for the peak of high-grade metamorphism in the KKB.

Table 1
Sm–Nd isotope data and calculated εNd and model ages for gneisses, granulites and granites of the KKB

Sample no.	Rock type	Sm (ppm)	Nd (ppm)	$^{147}Sm/^{144}Nd$	$^{143}Nd/^{144}Nd$ measured	2σ	$^{143}Nd/^{144}Nd$ (t = 550 Ma)	εNd	TDM (Ma)
K15-1	Augen gneiss	16.3	102	0.095972822	0.511188662	0.000013	0.5108428	−21.22	2458
K3	Garnet-biotite gneiss	1.89	12.2	0.093785724	0.511238344	0.000014	0.5109004	−20.10	2354
K3-6	Leucogranite	1.55	7.33	0.127900543	0.511405064	0.000014	0.5109442	−19.24	2966
199-66-9	Garnet-biotite gneiss	9.24	51.3	0.109000308	0.511182686	0.000017	0.5107899	−22.25	2760
199-66-8	Leucogranite	1.62	9.43	0.104129656	0.5114259	0.000021	0.5110507	−17.16	2318
100-8-3	Enderbite	10.5	61.8	0.102888506	0.511262933	0.000013	0.5108922	−20.26	2508
100-14-2	Metapelite	12.7	83.9	0.091413324	0.511190977	0.000012	0.5108616	−20.85	2367
MR 211	Charnockite	0.663	5.47	0.073226939	0.510922469	0.000010	0.5106586	−24.82	2351
199-48-2	Metabasite	0.380	1.59	0.144045552	0.511932497	0.000010	0.5114134	−10.07	2531
199-55-1	Charnockite	6.59	56.9	0.0699471	0.510890349	0.000034	0.5106383	−25.22	2332
199-55-3	Metabasite	4.08	16.0	0.154169922	0.512088834	0.000013	05115333	−7.734	2561
199-50-1	Charnockite	5.37	42.8	0.075838759	0.51101156	0.000006	0.5107383	−23.26	2299
199-50-2	Metabasite	6.53	37.8	0.1O4338O43	0.511413554	0.000019	0.5110376	−17.42	2339
199-63-3	Charnockite	5.79	60.2	0.05809249	0.510936262	0.000012	0.5107269	−23.49	2115
199-62-1	Charnockite	4.43	28.5	0.093983076	0.511118528	0.000009	0.5107799	−22.45	2504
199-51-1	Garnet-biotite gneiss	5.83	46.0	0.076560238	0.511069013	0.000016	0.5107931	−22.19	2249
199-57-1	Charnockite	4.90	37.3	0.079284772	0.510987409	0.000013	0.5107017	−23.98	2382
199-60-1	Garnet-biotite gneiss	1.83	10.5	0.105379961	0.511347728	0.000014	0.510968	−18.78	2449
100-18-2	Garnet-biotite gneiss	10.7	62.5	0.103520021	0.511226664	0.000010	0.5108536	−21.01	2570
100-18-3	Leucogranite	4.00	22.8	0.105924614	0.511482701	0.000016	0.511101	−16.18	2278
100-16-1	Garnet-biotite gneiss	9.45	52.6	0.108724528	0.511246949	0.000009	0.5108552	−20.98	2664
I00-15-5a	Enderbite	1.82	11.1	0.099356623	0.511341507	0.000019	0.5109835	−18.47	2333
I00-15-5b	Quartz-norite	3.54	18.8	0.114187469	0.511493531	0.000012	0.5110821	−16.55	2444
100-24-1	Enderbite	5.57	26.6	0.126673776	0.512194072	0.000012	0.5117376	−3.743	1610
100-28-1	Charnockite	10.8	64.4	0.10121748	0.512132635	0.000014	0.5117679	−3.151	1338

εNd at the time of metamorphism is calculated relative to CHUR with present-day values of $^{143}Nd/^{144}Nd = 0.512638$ and $^{147}Sm/^{144}Nd = 0.1967$ (Jacobsen and Wasserburg, 1980). Nd model ages (TDM) are calculated with a depleted-mantle reservoir and present-day values of $^{143}Nd/^{144}Nd = 0.51315$ and $^{147}Sm/^{144}Nd = 0.217$ (Goldstein et al., 1984).

In the PU and NU, gneisses, charnockites and enderbites are characterised by εNd values between −18 and −26. For leucogranites and metabasites, these values are less negative (−17 to −19 and −7 to −17, respectively). Corresponding Archean or Early Proterozoic model ages (TDM) range between 2.9–2.0 Ga and 2.4–2.0 Ga, respectively. A notable exception are two enderbite samples (I00-24-1 and I00-28-1) from the presumed southeastern continuation of the AU around Tirunelveli. They are characterised by lower model ages (TDM = 1.61 and 1.34 Ga respectively) and higher initial εNd (− 3.7 and −3.2 respectively) although Sm/Nd ratios are in the same range as all other samples.

In three localities (I99-48 and MR211; I99-55; I99-50) massive charnockites and associated metabasites were sampled. Only for a single charnockite-metabasite pair (I99-50), TDM and εNd are similar (2.32 ± 0.02 Ga and -20 ± 3 Ga respectively) although εNd of the metabasite is slightly higher. In the two other cases the metabasites (I99-48-2 and I99-55-3) yield model ages which are 180 or 230 Ma older and initial εNd values 14 or 18 εNd units less negative than the adjacent charnockite (−10.1 and −7.7 respectively). These two metabasites have high Sm/Nd ratios (up to 0.15). In three localities (I99-66; I00-18; K3) garnet-biotite gneisses and associated leucogranites were

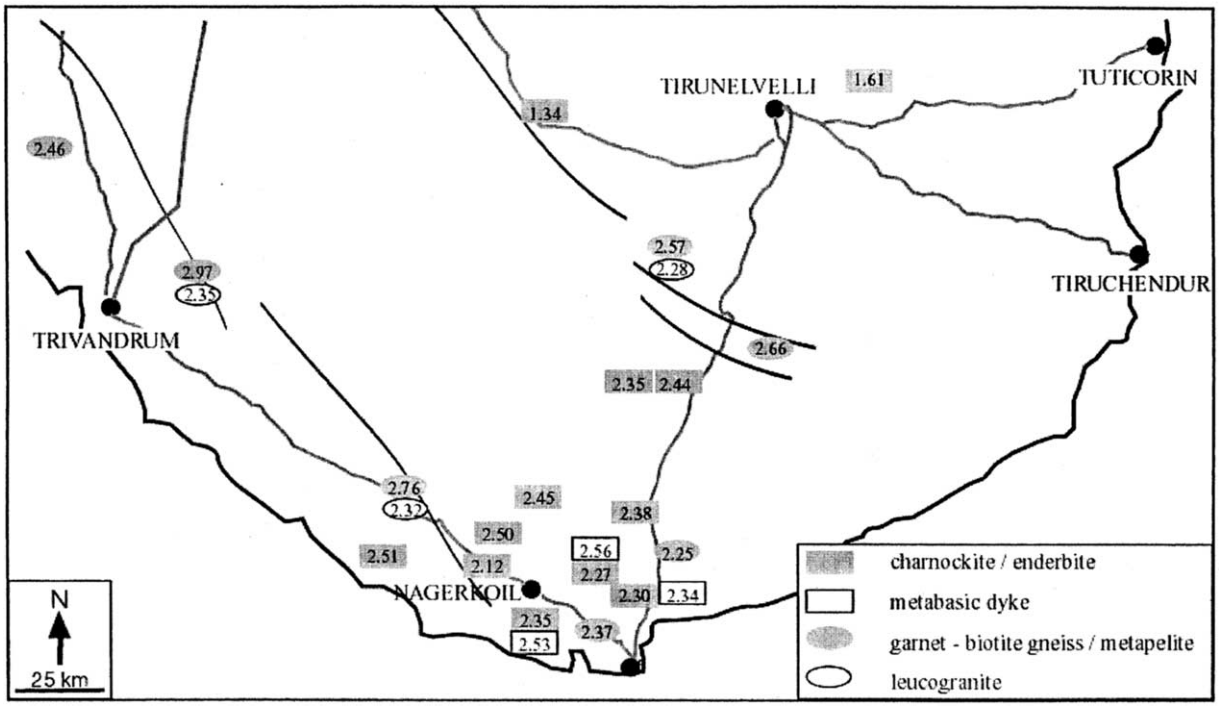

Fig. 2. Nd model ages map for all studied localities. Lithologies are also indicated.

investigated. TDM for leucogranites I99-66-8 and I00-18-3 are 300–450 Ma younger than their host rocks, the corresponding εNd values are about 5 units higher. TDM for leucogranite K3-6 is 600 Ma older than for the adjacent gneiss K3 and the corresponding εNd 0.9 units higher. However, Sm/Nd ratios are similar, indicating no major fractionation after segregation from depleted mantle. At locality I00-15, a garnet-bearing enderbite and a garnet-free quartz-norite were sampled. TDM of the garnet-bearing enderbite is 100 Ma younger and the corresponding εNd is 2 units lower compared to the garnet-free quartz-norite.

4.2. Geochronology: U–Pb and Rb–Sr dating

The results of U–Pb dating of monazites are listed in Table 2 and shown in Figs. 3 and 4. As is clear from Fig. 3, most of the studied monazites are discordant. Sample I99-65-1 is a garnet-biotite gneiss sampled within the PU. Three fractions yielded $^{207}Pb/^{235}U$ ages of 567 ± 2.5 (200–160 μm), 570 ± 2.4 (160–125 μm), 564 ± 3.1 Ma (125–100 μm), weighted mean = 567 ± 7.1 Ma. All fractions are slightly discordant reflecting Pb loss due to unidentified post-crystallisation processes. Sample I99-34-4 is a garnet-biotite gneiss sampled 30 km south of Tirunelveli within the PU. Three analysed size fractions yielded $^{207}Pb/^{235}U$ ages of 553 ± 2.1 (200–160 μm), 552 ± 2.7 (160–125 μm) and 549 ± 2.1 Ma (125–100 μm), weighted mean: 551 ± 5.5 Ma. These monazites are slightly reverse concordant indicating that excess ^{206}Pb, related to the decay of ^{230}Th, was incorporated in the monazite upon crystallisation (Schärer, 1984; Parrish, 1990). Sample I00-2-3 and 5 were collected in Pongamuda, an active quarry close to Trivandrum. I00-2-3 is a garnet-biotite gneiss and I00-2-5 is the adjacent massive charnockite. The largest grain size fraction of the charnockite is highly discordant and yields an age of 842 ± 3.9 Ma. Smaller grain size fractions from both samples are almost concordant (charnockite: 589 ± 2.4 Ma, 577 ± 2.4 Ma; gneiss: 580 ± 2.3 Ma).

Pegmatites are common and at the contact to charnockites fluid release from these melt injections

Table 2
U–Pb monazite data for selected gneiss and charnockite samples

Sample	Rock type	Size frac. (μm)	Weight (mg)*	Concentrations**		Atomic ratios					Apparent ages (Ma)		
				U (ppm)	Pb (ppm)	$^{206}Pb/^{204}Pb$	$^{208}Pb/^{206}Pb$	$^{207}Pb/^{206}Pb$	$^{207}Pb/^{235}U$	$^{206}Pb/^{238}U$	$^{206}Pb/^{238}U$	$^{207}Pb/^{235}U$	$^{207}Pb/^{206}Pb$
199-65-1	Garnet-biotite gneiss	125–100	0.033	7302	3791	3641	5.5105	0.05909 (1)	0.7421 (41)	0.0911 (5)	562	564	570
		160–125	0.067	8716	4566	7615	5.5113	0.05937 (1)	0.7527 (32)	0.0920 (3)	567	570	581
		200–160	0.092	8061	4147	17939	5.4474	0.05937 (1)	0.7472 (34)	0.0913 (4)	563	567	581
100-2-5	Charnockite	Small	0.044	11245	5902	6348	5.2558	0.05943 (1)	0.7854 (32)	0.0958 (4)	590	589	583
		Middle	0.067	6112	3259	14650	5.5140	0.05922 (1)	0.7645 (32)	0.0936 (4)	577	577	575
		Big	0.061	4082	2488	8092	4.7258	0.07723 (1)	1.2909 (60)	0.1212 (5)	738	842	1127
100-2-3	Garnet-biotite gneiss	Middle	0.097	4585	2350	6039	5.2366	0.05946 (1)	0.7697 (30)	0.0939 (3)	578	580	584
199-34-4	Garnet-biotite gneiss	125–100	0.044	3279	2194	6983	7.6074	0.05839 (1)	0.7174 (28)	0.0891 (3)	550	549	544
		160–125	0.075	4911	2810	5768	6.3061	0.05848 (2)	0.7224 (35)	0.0896 (3)	553	552	547
		200–160	0.107	4667	2826	8364	6.0811	0.05843 (1)	0.7244 (28)	0.0899 (3)	555	553	546

The isotopic ratios are corrected for fractionation, blank and common Pb. The errors on the isotopic ratios are given at the 2σ level (number in brackets indicates uncertainties on the last digits).

* Sample weight for all size fractions estimated from spheric shape and a specific weight of 5 g/cm.

** Only approximate concentrations due to uncertainties in sample weight.

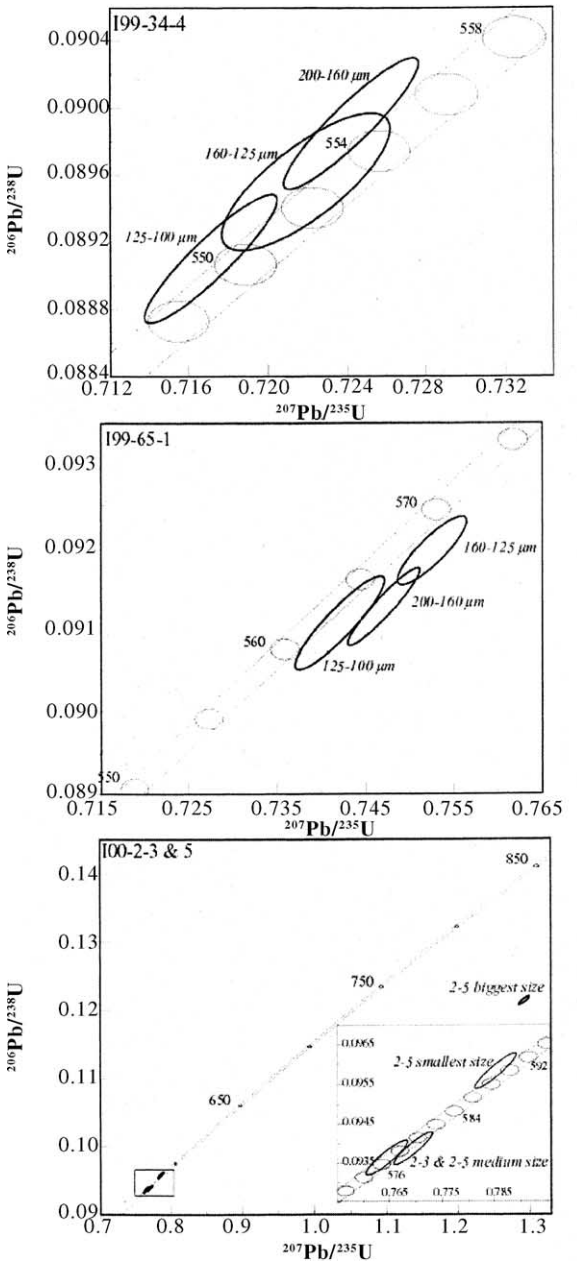

Fig. 3. Concordia diagram with U–Pb monazite data. For samples I00-2-3 and 5, only a relative grain size is available due to a small amount of material. Error ellipses are 2σ. Calculations and plotting are made with Isoplot version 2.49 (Ludwig, 1991).

often caused retrograde bleaching. In such zones, decimeter- to meter-sized amphibolite facies gneiss assemblage developed at the expense of the charnockite. Five pegmatite samples, which cross-cut massive charnockite, were selected for Rb–Sr dating of biotite and feldspars. Analytical results and ages are presented in Table 3 and Fig. 4. Biotite-feldspar ages range between 491 ± 10 Ma and 471 ± 4 Ma.

5. Discussion

5.1. Nd isotope characteristics

Garnet-biotite gneisses, metapelites and charnockites from the PU and the NU display the same range of mean crustal residence ages and εNd values. Based on a more comprehensive dataset, the results of this study confirm on a regional scale previous Nd isotope work and geochronology that was mainly focused on a smaller area north of Trivandrum (Harris et al., 1994; Brandon and Meen, 1995; Bartlett et al., 1998). Although rocks from the NU do not show TDM older than 2.4 Ga (Figs. 5 and 6), the regional distribution of calculated Nd model ages (Fig. 2) does not support a distinction between the PU and the NU as different age provinces. Since both units predominantly consist of rocks of sedimentary origin the Nd model ages have to be regarded as mean crustal residence ages. The observed similarity suggests that the protoliths most likely were derived from similar crustal basement areas. However, it cannot be completely ruled out that the observed range in Nd model ages reflects the addition of juvenile Proterozoic material. Our results show that young Nd model ages in the northernmost part of the KKB are not restricted to the cordierite gneisses alone, but also occur in a distinct crustal domain within the southernmost part of the SGT, which probably corresponds to the AU (Braun and Kriegsman, 2003). At this stage of our investigation, we have no convincing explanation for the much younger TDM ages of the AU. Brandon and Meen (1995) considered that the sedimentary protoliths in part originated from a much younger source which is only exposed in the Wanni Complex of Sri Lanka. Alternatively, these values could indicate addition of juvenile material or Sm/Nd fractionation during low-degree melt extraction. However, the distribution of Mesoproterozoic model ages does not coincide with the observed structural trends and the general strike (Cenki and Kriegsman, unpublished data). This feature of the study area is also known from the lower

Table 3
Rb–Sr isotope data from selected pegmatites of the KKB

Sample	Mineral	Concentrations (ppm)		Isotope ratios			Age (Ma)	$^{87}Sr/^{86}Sr_{initial}$
		Rb	Sr	$^{87}Rb/^{86}Sr$	$^{87}Sr/^{86}Sr$	2σ		
K12-2	Feldspar	445	247	5.275	0.853036	0.000015	476 ± 7	0.817278 ± 0.001196
	Biotite	1029	10	359.270	3.252496	0.000327		
100-2-2	Feldspar	97	690	0.406	0.720318	0.000009	480 ± 8	0.717544 ± 0.000060
	Biotite	1231	18	235.024	2.324091	0.000037		
100-12-1	Feldspar	136	518	0.759	0.735450	0.000012	471 ± 4	0.730360 ± 0.000105
	Biotite	1017	19	168.724	1.861558	0.000028		
100-10-3	Feldspar	641	356	5.241	0.753811	0.000138	474 ± 10	0.718406 ± 0.002961
	Biotite	1947	14	569.171	4.563605	0.000099		
100-7-2	Feldspar	546	87	18.735	1.005358	0.000018	491 ± 10	0.874154 ± 0.005855
	Biotite	1389	7	908.162	7.234216	0.000167		

Mineral ages are calculated using a Zentrallabor Labor fur Geochronologie shareware program.

crustal basement of Sri Lanka. Clearly, more detailed mapping and isotope studies are required to solve this problem.

The specific petrogenetic processes involved in the formation of leucogranites and two metabasites have caused modifications of their Nd isotope systematics. The high Sm/Nd ratios (up to 0.15) for metabasite samples I99-48-2 and I99-55-3 are either a primary feature related to high degree of partial melting in the mantle or influenced by the crystallisation and segregation of a LREE-rich mineral, that fractionates Nd rather than Sm (e.g. apatite). However, the metabasite I99-50-2 is not affected by fractionation of Nd over Sm and its εNd is lower than that for other rock types.

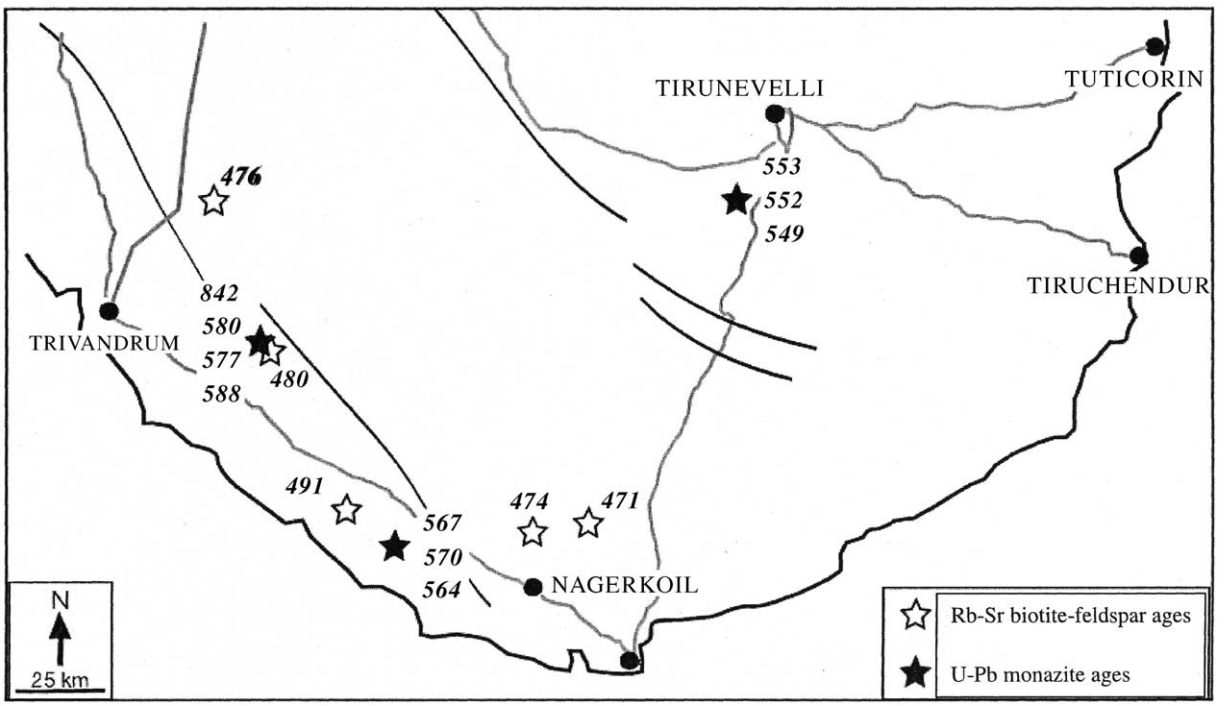

Fig. 4. Location map for geochronological results. Monazite U–Pb ages are presented from bigger to smaller grain size.

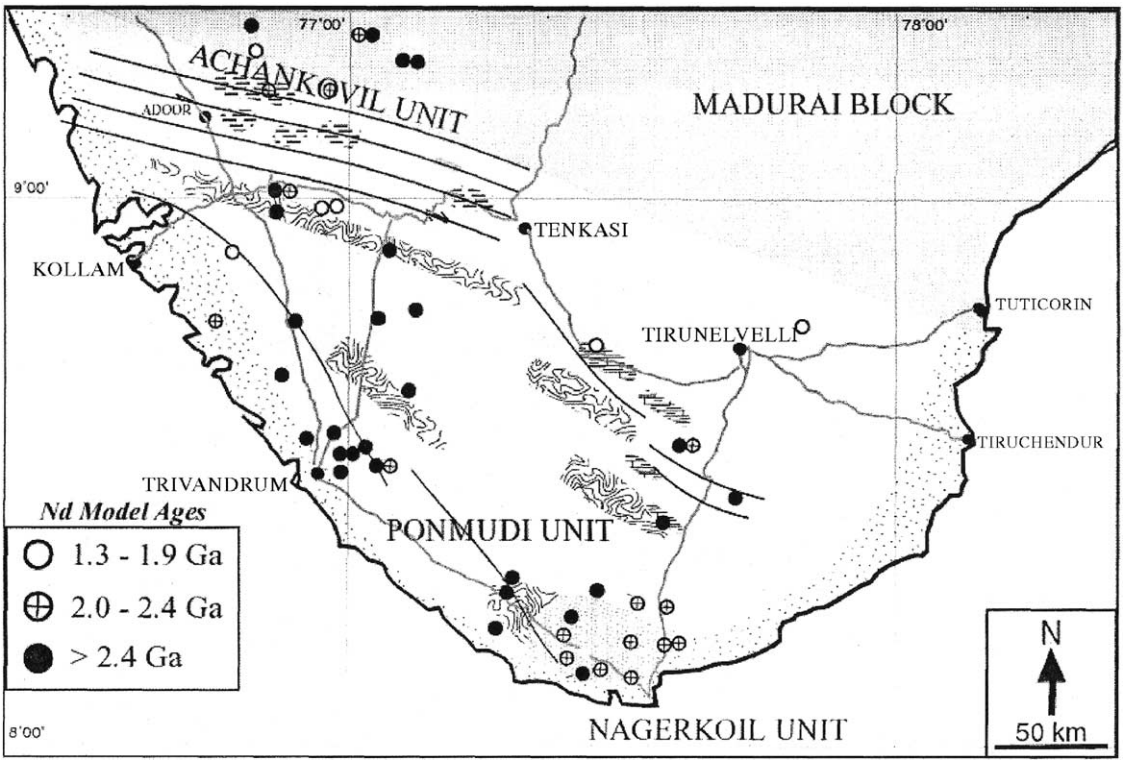

Fig. 5. Compilation map of all Nd model ages data available in literature for the Ponmudi Unit, the Achankovil Unit and the southern part of the Madurai Block in addition to the dataset performed in this study. Legend is similar to Fig. 1b.

Based on significantly different Sri ratios, Braun et al. (1996) showed that the leucogranites were not generated by in situ melting of the gneisses into which they were emplaced, but from compositionally similar gneisses with different Sr isotopic characteristics. Likewise, the leucogranites investigated in this study are also different in their Nd isotopic composition and yield Nd model ages that do not match those of their host rocks (Table 1), thus pointing to variations in the isotopic composition of the gneissic basement of the PU.

5.2. Geochronology

Monazite often yields concordant U–Pb dates (e.g. Parrish, 1990; Davis et al., 1994; Krogh and Moser, 1994), but this is not the case with the data presented in this study. Hawkins and Bowring (1997) and Catlos et al. (2002) offer a summary of the various phenomena that influence the U–Pb system and thus the concordancy of monazite: presence of an inherited component, protracted or episodic crystal growth, high temperature diffusive Pb loss, U–Th disequilibrium, fluid/mineral interaction, hydrothermal growth, and deformation. The investigated monazites are either reverse (I99-34-4), normal disconcordant (I99-65-1) or concordant (I00-2-3 and I00-2-5, small size fractions). In the reversely discordant results, the $^{207}Pb/^{235}U$ date is either a true age or it is affected by partial Pb loss and thus is only a minimum age. Interpretation of datasets including reversely discordant and concordant monazites is not straightforward. The apparently concordant dates may result from partial Pb loss of originally reversely discordant grains. Because the degree of reverse discordancy can also be reduced by partial Pb loss, all $^{207}Pb/^{235}U$ monazite dates of this study will be considered as minimum ages for crystallisation or closure during cooling.

In sample I00-2-5, the smaller grain sizes are analytically concordant whereas the largest is strongly

discordant. In addition, different size fractions for the same sample never coincide and differ by up to 10 Ma. The largest grain sizes did not always yield the oldest date (e.g. I00-2-5) suggesting episodic growth. The old date for the biggest monazite size fraction from the charnockite sample I00-2-3 indicates the presence of an inherited component. Ghosh (1999) reports a 987 Ma zircon upper intercept age for a gneiss xenolith in the Kalipara granite (western Achankovil Unit). Similarly, the older inherited component recognised in sample I00-2-3 is likely to be of Grenvilian age.

The ages of the studied samples only provide a minimum estimate for the timing of the thermal peak because the temperature maximum in the KKB reached values up to 950 °C (Nandakumar and Harley, 2000; Cenki et al., 2002), clearly above the closure temperature for monazite. As also shown by other datasets (Braun and Bröcker, 2004), Pan-African ages of the KKB show a considerable range between 590 and 520 Ma. The fact that there are old ages preserved, coupled with the lack of correlation between grain size and age suggests that monazite formation and/or variable degrees of recrystallization occurred at different stages of a protracted metamorphic evolution. These processes can either be related to temperature variations caused by thermal pulses at local or crustal scale, to fluid infiltration or to changes in melt composition (e.g. local variation of water activity, concentration in P and LREE).

Rb–Sr ages of pegmatites (470 and 490 Ma) constrain the cooling path. Judging from the large centimeter-sized biotite crystals, a higher closure temperature (ca. 400–500 °C) appears to be more reasonable than the commonly quoted value of 350 °C (±50).

Based on these data, we may roughly estimate the cooling rate of the KKB subsequent to Pan-African high-grade metamorphism. Our results of U–Pb (590–550 Ma) and Rb–Sr dating (490–470 Ma) yield Δt values between 60 and 120 Ma. The corresponding ΔT is calculated from closure temperature (Tc) estimates for Pb diffusion in monazite (725–780 °C; Copeland et al., 1988; Parrish, 1990; Dahl, 1990) and Sr diffusion in biotite (400–500 °C) and ranges between 225 and 380 °C. Combining maximum and minimum values for Δt and ΔT yields cooling rates of 1.9–6.3 °C/Ma.

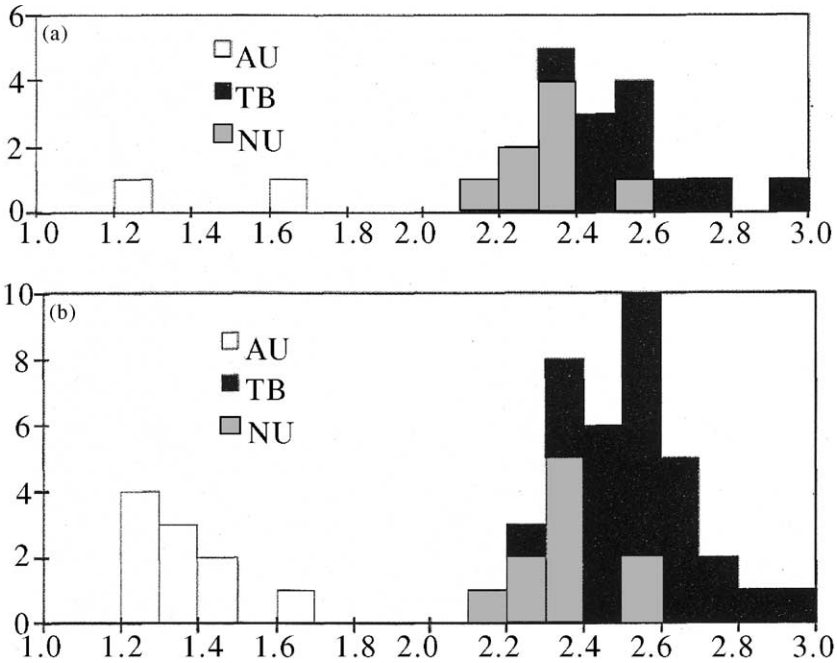

Fig. 6. Histogram of all Nd model ages data available in literature (b) for the Ponmudi Unit, the Achankovil Unit and the southern part of the Madurai Block in addition to the dataset performed in this study (a).

Clearly, these calculations are very simplistic and unless the different stages of the tectono-metamorphic evolution are precisely dated only provide a first guess on the uplift of the KKB. However, even if we take higher and lower values for T_c^{Pb} and T_c^{Sr}, respectively, the corresponding cooling rates would not exceed 8–8.5 °C/Ma. We therefore infer that the KKB experienced slow cooling from ultra-high to high temperatures and most likely prevailed at lower crustal conditions for at least 70 Ma. This assumption is in fairly good agreement with recent investigations on the P-T evolution of the KKB (Satish Kumar and Harley, 1998; Nandakumar and Harley, 2000; Cenki et al., 2002) who propose near-isobaric cooling at granulite-facies conditions.

5.3. Regional implications

The isotope geochemical and geochronological data presented in this study do not only serve to understand the origin and magmatic-metamorphic evolution of the major rock types of the KKB more comprehensively, but also help to refine its position within Gondwana at the end of the Proterozoic. Although the database for the MB is fairly limited, the range covered by Nd model ages, U–Pb zircon and monazite and Rb–Sr ages are apparently similar to the data from the KKB presented here and in other studies (Braun and Kriegsman, 2003 and ref. therein). This and the absence of a suture between the KKB and the MB make it very likely that both terrains shared a common Pan-African tectono-metamorphic evolution and were in a neighbouring position during Gondwana assembly at the end of the Proterozoic. Nd model ages younger than 2.0 Ga were reported by Meissner et al. (2002) from the southern part of the Palghat-Cauvery Shear Zone. However, a metasedimentary unit with Middle Proterozoic crustal residence ages (Achankovil Unit) is not known from the MB. Nevertheless, the available information points to a large composite crustal terrain whose sedimentary protoliths were derived from different source regions of predominantly Early Proterozoic and Late Archaean age. The age of sedimentation is unknown.

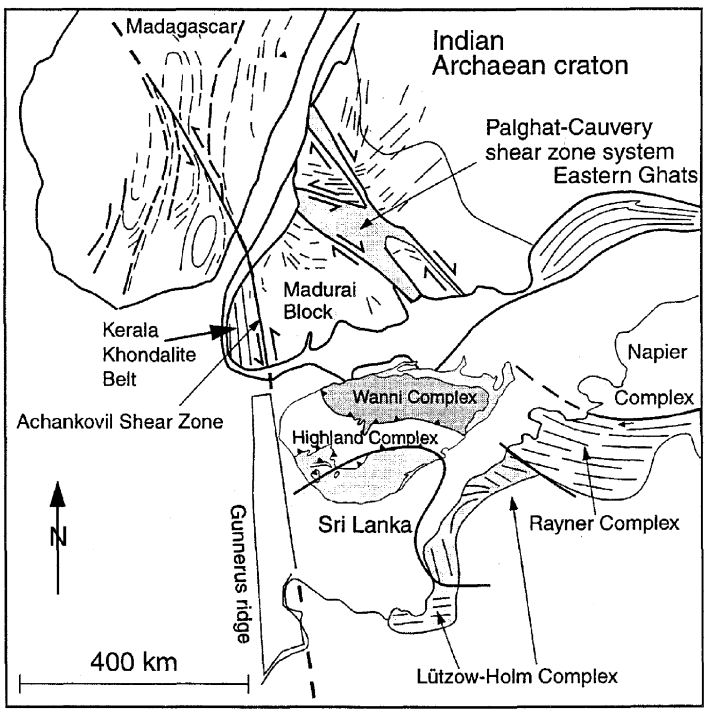

Fig. 7. Gondwana reconstruction showing the position of southernmost India, Sri Lanka and southern Madagascar (modified after Kriegsman, 1995; Kröner et al., 2000).

Commonly, Gondwana reconstructions show Peninsular India in close spatial relationship to the lower crustal terrains of Sri Lanka and southern Madagascar (Fig. 7). The Highland Complex of Sri Lanka forms a crustal unit which is predominantly composed of metasediments. Nd mean crustal residence ages of 2.0–3.0 Ga and U–Pb zircon ages of ca. 550 Ma overlap very well with data from the MB and the KKB (Hölzl et al., 1991). The same holds true for the available P-T data and inferred P-T path reconstructions (Schumacher and Faulhaber, 1994; Raase and Schenk, 1994) upon which a correlation with the PU and the granulite-facies parts of the MB has been suggested (Braun and Kriegsman, 2003). In contrast, the Wanni Complex (WC) of Sri Lanka is mainly made up of granitic and metasedimentary gneisses. Cordierite-rich gneisses similar to the ones known from the AU form a prominent litho-unit of the south-western part of this unit (Milisenda et al., 1988, 1994; Prame and Pohl, 1994). Available Nd model ages range between 1.0 and 2.0 Ga. They are significantly younger than those of the Highland Complex and its tentative counterparts in Peninsular India, but comparable to ages reported from the AU. It thus suggests that a possible linkage exists between the Wanni Complex and the AU (Braun and Kriegsman, 2003).

The Precambrian basement of southern Madagascar most likely was juxtaposed to southern India at the end of the Proterozoic. This view has been inferred from similarities in structural features, P-T evolution and lithology, particularly the occurrence of cordierite gneisses along the Ranotsara and the Achankovil Shear Zones, which were regarded as parts of an intra-crustal mega-shear zone (Nicollet, 1990, Windley et al., 1994, Markl et al., 2000; De Wit et al., 2001). Furthermore, the available Nd model ages (2.8–2.1 Ma) and the geochronological data provide strong evidence for a common tectono-metamorphic history of both terrains during the Proterozoic (Paquette et al., 1994). Accordingly, high-grade metamorphism in southern Madagascar started 650–630 Ma ago (De Wit et al., 2001). Currently available data for the KKB indicate that granulite-facies conditions were reached at least 590 Ma ago (Braun and Bröcker, 2004). However, it should be noted that the reverse discordant U–Pb monazite ages presented in this study, and also discussed by Braun and Bröcker (2004) for the central and northern part of the KKB, represent minimum ages. Thus granulite facies metamorphism in the KKB might have started much earlier and the time interval between the peak metamorphism in Madagascar and the KKB is probably smaller than commonly thought. The post-peak metamorphic stage in southern Madagascar and Peninsular India is characterized by very slow cooling (Madagascar: 1–2 °C/Ma, Ashwal et al., 1999; India: 2–6 °C/Ma, this study) until temperatures below the closure temperature for Sr diffusion in biotite and feldspar were achieved ca. 480–450 Ma ago.

6. Conclusions

The results of this study confirm previous interpretations related to the crustal evolution and timing of metamorphism in the KKB (Brandon and Meen, 1994, Harris et al., 1994, Soman et al., 1995, Miller et al., 1997, Bartlett et al., 1998). Charnockites and garnet-biotite gneisses yield Nd model ages between 3.0 and 2.0 Ga in the entire area, except in the AU where TDM are much younger (1.6–1.3 Ga). The KKB in Eastern Gondwana is dominated by Late Archean and Early Proterozoic Nd model ages. U–Pb monazite geochronology brackets the timing of high-temperature metamorphism between 590 and 550 Ma. Biotite-feldspar pairs of pegmatites yielded Rb–Sr ages between 470 and 490 Ma which are interpreted as time constraints for cooling below ca. 400–500 °C. Thus, very slow cooling (<6 °C/Ma) is likely for the KKB, similar to what has been inferred for Madagascar and Sri Lanka.

Acknowledgements

We thank Dr. G.R.R. Ravindra Kumar for precious help during fieldwork. B.C. thanks H. Baier, U. Lange and the helpful team of the Münster laboratory. B.C. is specially grateful to K. Mezger for precious help and discussions during laboratory work. B.C. thanks J.-E. Martelat for discussions on shear zones and Madagascar. Research was financially supported by the Deutsche Forschungsgemeinschaft (DFG), the Deutscher Akademischer Austauschdienst (DAAD) and the Zentrallabor für Geochronologie. The paper benefited significantly from constructive reviews from John Percival and Somnath Dasgupta.

References

Ashwal, L.D., Tucker, R.D., Zinner, E.K., 1999. Slow cooling of deep crustal granulites and Pb-loss in zircon. Geochim. et Cosmochim. Acta 63 (18), 2839–2851.

Bartlett, J.M., Dougherty-Page, J.S., Harris, N.B.W., Hawkesworth, C.J., Santosh, M., 1998. The application of single zircon evaporation and Nd model ages to the interpretation of polymetamorphic terrains: an example from the Proterozoic mobile belt of south India. Contrib. Miner. Petrol. 131, 181–195.

Brandon, A.D., Meen, J.K., 1995. Nd isotopic evidence for the position of southernmost Indian terranes within East Gondwana. Precambrian Res. 70, 269–280.

Braun, I., Bröcker, M., 2004. Monazite dating of granitic gneisses and leucogranites from the Kerala Khondalite Belt, southern India: implications for Late Proterozoic crustal evolution in East Gondwana. Intl. J. Earth Sci. 93, 13–22.

Braun, I., Kriegsman, L.M., 2003. Proterozoic crustal evolution of southernmost India and Sri Lanka. In: Yoshida, M., Windley, B.F. (Eds.), Proterozoic East Gondwana: Supercontinents Assembly and Breakup. Special Publications, Geological Society, London, pp. 169–203.

Braun, I., Montel, J.-M., Nicollet, C., 1998. Electron microprobe dating of monazites from high-grade gneisses and pegmatites of the Kerala Khondalite Belt, southern India. Chem. Geol. 146, 65–85.

Braun, I., Raith, M., Ravindra Kumar, G.R., 1996. Dehydration-melting phenomena in leptynitic gneisses and the generation of leucogranites: a case study from the Kerala Khondalite Belt, southern India. Journal of Petrology. 37, 1285–1305.

Buhl, D., 1987. U–Pb und Rb–Sr-Altersbestimmungen und Untersuchungen zum Strontiumisotopenaustausch an Granuliten Südindiens. Unpublished Ph.D. Thesis, Universität Münster.

Catlos, E.J., Gilley, L.D., Harrison, T.M., 2002. Interpretation of monazite ages obtained via in situ analysis. Chem. Geol. 188, 193–215.

Cenki, B., Kriegsman, L.M., Braun, I., 2002. Melt-producing and melt-consuming reactions in the Achankovil cordierite gneisses, South India. J. Metamorphic Geol. 20, 543–561.

Cenki, B., Kriegsman, L.M., 2004. Tectonics of the Neoproterozoic Southern Granulite Terrane, south India. Precambrian Res., submitted for publication.

Chacko, T., Ravindra Kumar, G.R., Meen, J.K., Rogers, J.J., 1992. Geochemistry of high-grade supracrustal rocks from the Kerala Khondalite Belt and adjacent massif charnockites. South India. Precambrian Res. 55, 469–489.

Chacko, T., Lamb, M., Farquhar, J., 1996. Ultra-high temperature metamorphism in the Kerala Khondalite Belt. In: Santosh, M., Yoshida, M. (Eds.), The Archaean and Proterozoic Terrains in Southern India within East Gondwana, 3. Gondwana Research Group Memoir, pp. 157–165.

Choudhary, A.K., Harris, N.B.W., Van Calsteren, P., Hawkesworth, C.J., 1992. Pan-African charnockite formation in Kerala, South India. Geol. Mag. 129, 257–264.

Collins, A.S., Windley, B.F., 2002. The tectonic evolution of central and northern Madagscar and its place in the final assembly of Gondwana. J. Geol. 110, 325–339.

Davis, D.W., Schandl, E.S., Wasteneys, H.A., 1994. U–Pb dating of minerals in alteration halos of Superior Province massive sulfide deposits: syngenesis versus metamorphism. Contrib. Miner. Petrol. 115, 427–437.

De Wit, M.J., Bowring, S.A., Ashwal, L.D., Randrianasolo, L.G., Morel, V.P.I., Rambeloson, R.A., 2001. Age and tectonic evolution of Neoproterozoic ductile shear zones in southwestern Madagascar, with implications for Gondwana studies. Tectonics 20 (1), 1–45.

Drury, S.A., Holt, R.W., 1980. The tectonic framework of the South Indian craton: a reconnaissance involving LANDSAT imagery. Tectonophysics 65, 5.

Drury, S.A., Harris, N.B.W., Holt, R.W., Reeves-Smith, G.W., Wightman, R.T., 1984. Precambrian tectonics and crustal evolution in South India. J. Geol. 92, 1–20.

Fitzsimons, I.C.W., 2000. A review of tectonic events in the Eastern Antarctic shield and their implications for Gondwana and earlier supercontinents. J. Afr. Earth Sci. 31, 3–23.

Fonarev, V.I., Konilov, A.N., Santosh, M., 2000. Multistage metamorphic evolution of the Trivandrum Granulite Block, southern India. Gondwana Res. 3, 293–314.

Ghosh, J.P., Zartman, R.E., De Wit, M.J., 1998. Re-evaluation of tectonic framework of southernmost India: new U–Pb geochronological and structural data, and their implication for Gondwana reconstruction. In: Almond, J., Anderson, J., Booth, P., Chinsamy-Turan, A., Cole, D., de Wit, M.J., Rubridge, B., Smith, R., Storey, B.C., Van Bever Donker, J. (Eds.), Gondwana 10: Event Stratigraphy of Gondwana; J. Afr. Earth Sci. 27/1A, 86.

Ghosh, J.P., 1999. U–Pb geochronology and structural geology across major shear zones of the Southern Granulite Terrain of India and organic carbon isotope stratigraphy of the Gondwana coal basins of India: their implications for Gondwana studies. Unpublished Ph.D., University of Cape Town, South Africa.

Goldstein, S.L., O'Nions, R.K., Hamilton, P.J., 1984. A Sm–Nd isotopic study of atmospheric dusts and particulates from major river systems. Earth Planet. Sci. Lett. 70, 221–236.

Harris, N.B.W., Santosh, M., Taylor, P.N., 1994. Crustal evolution in South India: constraints from Nd isotopes. J. Geol. 102, 139–150.

Hawkins, D.P., Bowring, S.A., 1997. U–Pb systematics of monazite and xenotime: case studies from the Paleoproterozoic of the Grand Canyon, Arizona. Contrib. Miner. Petrol. 127, 87–103.

Hiroi, Y., Motoyoshi, Y. (Eds.), 1990. Study of geologic correlation between Sri Lanka and Antarctica (1988–1989). Chiba University, Japan, p. 151.

Hölzl, S., Köhler, H., Kröner, A., Jaeckel, P., Liew, T.C., 1991. Geochronology of the Sri Lankan basement. In: Kröner, A. (Ed.), The crystalline crust of Sri Lanka. Part 1. Summary of Research of the German-Sri Lankan Consortium. Geological Survey Department of Sri Lanka, 5. Professional Paper, pp. 237–257.

Jacobsen, S.B., Wasserburg, C.J., 1980. Sm–Nd isotopic evolution on chondrites. Earth Planet. Sci. Lett. 50, 139–155.

Jahn, B.M., Condie, K.C., 1995. Evolution of the Kaapvaal Craton as viewed from geochemical and Sm–Nd isotopic analyses of intracratonic pelites. Geochem. Cosmochim. Acta 59, 2239–2258.

Kriegsman, L.M., 1995. The Pan-African event in East Antarctica: a view from Sri Lanka and the Mozambique Belt. In: Dirks,

P.H.G.M., Passchier, C.W., Hoek, J.D. (Eds.), Tectonics of East Antarctica, 75. Precambrian Res., pp. 263–277.

Kröner, A., Hergner, E., Collins, A.S., Windley, B.F., Brewer, T.S., Razakamanana, T., Pidgeon, R.T., 2000. Age and magmatic history of the Antananarivo Block, Central Madagascar, as derived from zircon geochronology and Nd isotope systematics. Am. J. Sci. 300, 251–288.

Krogh, T.E., 1973. A low contamination method for hydrothermal decomposition of zircon and extraction of U and Pb for isotopic age determinations. Geochim. Cosmochim. Acta 37, 485–494.

Krogh, T.E., Moser, D.E., 1994. U–Pb zircon and monazite ages from the Kapuskasing uplift: age constraints on deformation within the Ivanhoe Lake fault zone. Can. J. Earth Sci. 31, 1096–1103.

Lawver, L.A., Scotese, C.R., 1987. A revised reconstruction of Gondwanaland. In: McKenzie, G.D. (Ed.), Gondwana Six: Structure, Tectonics, and Geophysics, 40. American Geophysical Union, Geophysical Monograph, pp. 17–23.

Ludwig, K.R., 1991. ISOPLOT; a plotting and regression program for radiogenic-isotope data; version 2.53. U. S. G. S. Open File Rept., 91–0445.

McCullogh, M.T., 1987. Sm–Nd isotopic constraints on the evolution of Precambrian crust in the Australian continent. In: Kröner, A. (Ed.), Proterozoic Lithospheric Evolution. Geodynamic Series 17. American Geophysical Union, Washington, DC, pp. 115–130.

Markl, G., Bäuerle, J., Grujic, D., 2000. Metamorphic evolution of Pan-African granulite facies metapelites from southern Madagascar. Precambrian Res. 102, 47–68.

Milisenda, C.C., Liew, T.C., Hofmann, A.W., Kröner, A., 1988. Isotopic mapping of age provinces in Precambrian high-grade terrains: Sri Lanka. J. Geol. 96, 608–615.

Milisenda, C.C., Liew, T.C., Hofmann, A.W., Köhler, H., 1994. Nd isotopic mapping of the Sri Lanka basement: update, and additional constraints from Sr isotopes. In: Raith, M., Hoernes, S. (Eds.), Tectonic, Metamorphic, Isotopic Evolution of Deep Crustal Rocks, with Special Emphasis in Sri Lanka, 66. Precambrian Res., pp. 95–110.

Miller, J.S., Santosh, M., Pressley, R.A., Clements, A.S., Rogers, J.J.W., 1997. A Pan-African thermal event in southern India. J. Southeast Asian Earth Sci. 14, 127–136.

Nandakumar, V., Harley, S.L., 2000. A reappraisal of the Pressure-Temperature Path of Granulites from the Kerala Khondalite Belt, southern India. J. Geol. 108, 687–703.

Nicollet, C., 1990. Crustal evolution of the granulites of Madagascar. In: Vielzeuf, D., Vidal, P. (Eds.), Granulites and Crustal Evolution, pp. 291–310.

Paquette, J.-L., Nédélec, A., Moine, B., Rakotondrazafy, M., 1994. U–Pb, single zircon Pb-evaporation, and Sm–Nd isotopic study of a granulite domain in SE Madagascar. J. Geol. 102, 523–538.

Parrish, R.R., 1990. U–Pb dating of monazite and its application to geological problems. Can. J. Earth Sci. 27, 1431–1450.

Powell, C.McA., Roots, S.R., Veevers, J.J., 1988. Pre-breakup continental extension in East Gondwanaland and the early opening of the eastern Indian Ocean. Tectonophysics 155, 261–283.

Prame, W.K.B.N., Pohl, J., 1994. Geochemistry of pelitic and psammopelitic Precambrian metasediments from southwestern Sri Lanka: implications for two contrasting source terrains and tectonic settings. In: Raith, M., Hoernes, S. (Eds.), Tectonic, Metamorphic and Isotopic Evolution of Deep Crustal Rocks, with Special Emphasis on Sri Lanka, 66. Precambrian Res., pp. 223–244.

Raase, P., Schenk, V., 1994. Petrology of granulite-facies metapelites of the Highland Complex. In: Raith, M., Hoernes, S. (Eds.), Tectonic, Metamorphic and Isotopic Evolution of Deep Crustal Rocks, with Special Emphasis on Sri Lanka, 66. Precambrian Res., pp. 265–294.

Raith, M., Karmakar, S., Brown, M., 1997. Ultra-high-temperature metamorphism and multistage decompressional evolution of sapphirine granulites from the Palni Hills Ranges, southern India. J. Metamorphic Geol. 15, 379–399.

Ravindra Kumar, G.R., Chacko, T., 1986. Mechanisms of charnockite formation and breakdown in southern Kerala; implications for the origin of the southern Indian granulite terrain. J. Geol. Soc. India 28, 277–288.

Santosh, M., Yoshida, M., 1986. Charnockite in the breaking: evidence from the Trivandrum region, Kerala. J. Geol. Soc. India 28, 306–310.

Santosh, M., 1996. The Trivandrum and Nagercoil granulite blocks. In: Santosh, M., Yoshida, M. (Eds.), The Archaean and Proterozoic terrains in southern India within East Gondwana, 3. Gondwana Research Group Memoir, pp. 243–277.

Santosh, M., Yokoyama, K., Biju-Sekhar, S., Rogers, J.J.W., 2003. Multiple tectonothermal events in the granulite blocks of southern India revealed from EPMA dating: Implications on the history of supercontinents. Gondwana Research 6, 29–63.

Satish Kumar, M., Harley, S.L., 1998. Reaction textures in scapolite-wollastonite-grossular calc-silicate rock from the Kerala Khondalite Belt, southern India: evidence for high-temperature metamorphism and initial cooling. Lithos 44, 83–99.

Schärer, U., 1984. The effect of initial ^{230}Th disequilibrium on young U–Pb ages: the Malaku case, Himalaya. Earth Planet. Sci. Lett. 67, 191–204.

Schumacher, R., Faulhaber, S., 1994. Summary and discussion of P-T estimates from garnet-pyroxene-plagioclase-quartz-bearing granulite-facies rocks from Sri Lanka. In: Raith, M., Hoernes, S. (Eds.), Tectonic, Metamorphic and Isotopic Evolution of Deep Crustal Rocks, with Special Emphasis on Sri Lanka, 66. Precambrian Res., pp. 295–308.

Soman, K., Nair, N.G.K., Golubyev, V.N., Arakelyan, M.M., 1982. Age data on pegmatites of south Kerala and their tectonic significance. J. Geol. Soc. India 23, 458–462.

Soman, K., Narayanaswamy, Van Schmus, W.R., 1995. Preliminary U–Pb zircon ages of high-grade rocks in southern Kerala, India. J. Geol. Soc. India 45, 127–136.

Srikantappa, C., Raith, M., Spiering, B., 1985. Progressive charnockitization of a leptynite-khondalite suite in southern Kerala, India - evidence for formation of charnockites through decrease in fluid pressure? J. Geol. Soc. India 26, 849–872.

Steiger, R.H., Jäger, E., 1977. Subcommission on geochronology: convention on the use of decay constants in geo- and cosmochronology. Earth Planet. Sci. Lett. 36, 359–362.

Stacey, J.S., Kramers, J.D., 1975. Approximation of terrestrial lead isotope evolution by a two stage model. Earth Planet. Sci. Lett. 26, 207–221.

Unnikrishnan-Warrier, C., 1997. Isotopic signature of Pan-African rejuvenation in the Kerala Khondalite Belt, southern India: implications for East Gondwana Reassembly. J. Geol. Soc. India 50, 179–190.

Unnikrishnan-Warrier, C., Santosh, M., Yoshida, M., 1995. First report of Pan-African Sm–Nd and Rb–Sr mineral ages from regional charnockites of southern India. Geol. Mag. 132, 253–260.

Windley, B.F., Razafiniparany, A., Razakamanana, T., Ackermand, D., 1994. Tectonic framework of the Precambrian of Madagascar and its Gondwana connections: a review and reappraisal. Geol. Rundschau 83, 642–659.

Yoshida, M., Funaki, M., Vitanage, P.W., 1992. Proterozoic to Mesozoic East Gondwana: the juxtaposition of India, Sri Lanka, and Antarctica. Tectonics 11, 381–391.